

論文内容の要旨

論文題目 Study of Reversible Photo- and Electro- Isomerization Systems of Benzodimethyldihydropyrene Derivatives

(ベンゾジメチルジヒドロピレン類を用いた可逆な光・電気化学異性化反応系の研究)

氏名 岸田 正彬

Introduction

Photochromic molecules change their molecular structures and colors by light irradiation, thereby forming two metastable isomers. The photoisomerization accompanies the change of the molecule's electronic structure and physical properties, such as luminescence, magnetism, and electronic conductivity, and it is useful to combine the photo-functionality with the electro-functionality for the purpose to fabricate molecular devices. In this sense, to find unique electrochemical properties of photochromic molecules is important to establish dual electro- and photo responsive systems. In my Ph.D course study, I focused on benzodimethyldihydropyrene (BzDHP) derivatives. Benzodimethyldihydropyrene is one of the most efficient photochromic molecules; upon visible light irradiation, purple-colored, BzDHP, is transformed into a colorless benzocyclophanedine, BzCPD. The reverse isomerization is induced by UV light irradiation or heat treatment. It was known that BzDHP and BzCPD exhibited different redox properties, but the relationship between the photoisomerization and the redox properties have not been clarified. I discovered a new type of isomerization which is induced by oxidation, which allowed to fabricate both photo- and electro-responsive molecular modified electrode.

Electronic communication behavior of DHP between the ferrocene moieties and its electronic state

In chapter 2, I studied about the electronic state of DHP structure as spacer unit with comparing three molecules

(Figure 1). Previously it is known that **2** shows the electronic communication between two ferrocene. But the

electronic communication was confirmed by only cyclic voltammetry measurement. In order to reveal the effect of \square conjugation of the linker, I measured the UV-vis-NIR spectrometry and carried out DFT calculation to the three molecules. When an oxidant, $[(4\text{-BrC}_6\text{H}_4)_3\text{N}][\text{SbCl}_6]$, was added into the dichloromethane solution of **2**, UV-vis-NIR spectrum showed the broad band in the NIR region. This band is considered to compose of two different bands; the first band is an intervalence charge transfer transition from the ferrocene moiety to the ferrocenium moiety, and the second band is a charge transfer transition from the DHP moiety to the ferrocene moiety. This spectrum confirms the electronic

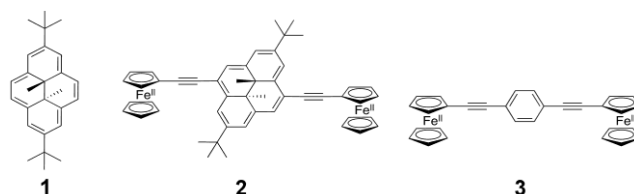


Figure 1. Molecule structure of 1-3.

communication between the two ferrocene in **2**. DFT calculation revealed the energy level of MOs as shown in Figure 2A. The energy level of the \square orbital of DHP is near that of d orbital of ferrocene, while the energy level of the \square orbital of diethynylphenylene is far from that of d orbital of ferrocene. These different energy diagrams support that DHP structure enhances the electronic interaction between

ferrocenes. These results suggest the \square conjugation of the linker is important to communicate the two redox active parts.

Fabrication of a modified electrode with reversible photo- and electro- responsive BzDHP molecules

I examined the photoisomerization of **4c** and **5c** on an ITO electrode (Figure 3). The modified electrode ITO-**4c** and ITO-**5c** was fabricated by immersing an ITO electrode into a 0.1 mM chloroform solution of **4c** for over night, in that of **5c** for 1h. The immobilization of **4c** and **5c** were confirmed by

cyclic voltammetry and UV-vis spectrometry. The reversible isomerization of ITO-**4c** was not observed, but that of ITO-**5c**

was observed. Figure 4A shows the cyclic voltammogram of ITO-**5c** after the visible light irradiation ($\lambda = 550$ nm). After the several redox reactions, the oxidation peak was observed at 0.30 V vs. Ag^+/Ag . The change of the voltammogram by the oxidation was similar to that observed in the cyclic

voltammogram of **5o** dissolved in a dichloromethane solution. This suggests that the same oxidation-induced cyclization of **5o** occurred for a molecule immobilized on ITO.

The UV-vis spectral change was observed by the 550 nm visible light irradiation as displayed in Figure 4B, where the peak absorbance at 400 nm was decreased. The following oxidation and the reduction of **5o** recovered the absorbance at 400 nm partially. These results suggest that visible light photoirradiation change ITO-**5c** to ITO-**5o** and the oxidation of

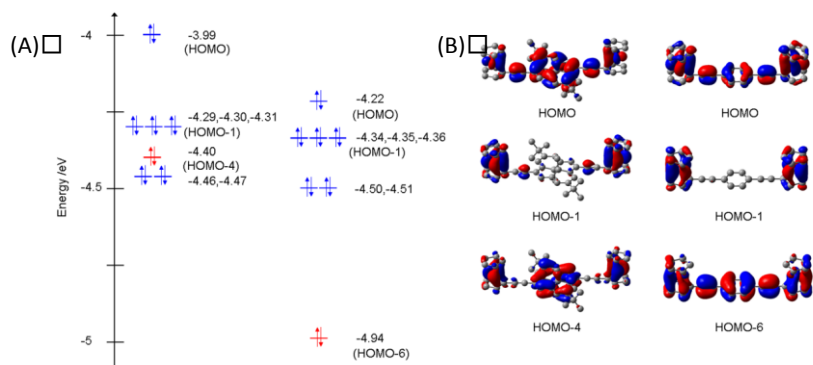


Figure 2. (A) Energy levels of HOMOs of **2** and **3** estimated by DFT calculation. The blue orbitals have d-orbital characters, whereas the red ones are chiefly composed of the \square orbitals of the linkers. (B) Selected molecular orbitals of **2** and **3**.

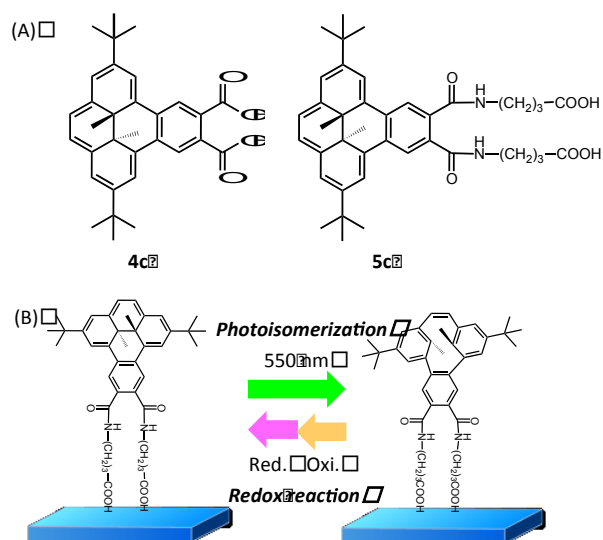


Figure 3. (A) Structure of **4c** and **5c** (B) Scheme of ITO-**5c** and ITO-**5o**.

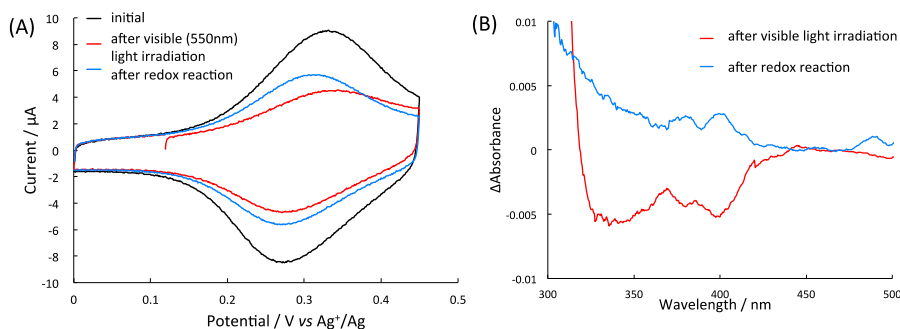


Figure 4. (A) Cyclic voltammograms of ITO-**5o** in the first scan (plain line) and in the second scan (dashed line) in 0.1 M Bu_4NClO_4 – dichloromethane. (B) Changes of Δ Absorbance after visible light irradiation (plain line) and after oxidation (dashed line). Δ Absorbance indicates difference of spectrum from a spectrum before the photoirradiation or oxidation.

$5\mathbf{o}^+/5\mathbf{o}$ change ITO- $5\mathbf{o}$ to ITO- $5\mathbf{o}$ as confirmed by the cyclic voltammograms.

Reversible potential switching based on DHP to CPD photoisomerization and electro-catalytic reverse isomerization

In chapter 4, I studied the photochemical and electrochemical properties of $6\mathbf{c}$, $6\mathbf{o}$ and their analogs $7\mathbf{c}$, $7\mathbf{o}$ (Figure 5). Figure 6 shows the cyclic voltammograms of $6\mathbf{c}$, $6\mathbf{o}$, $7\mathbf{c}$, and $7\mathbf{o}$. An irreversible redox wave was observed at $E_{p,a} = 0.39$ V (0.44 V) vs. ferrocenium/ferrocene in the cyclic voltammogram of $6\mathbf{o}$ ($7\mathbf{o}$), indicating an occurrence of a chemical process followed by oxidation (EC reaction). In the reverse scan in the negative direction, a cathodic peak was observed at the similar potential to that of $6\mathbf{o}$ ($7\mathbf{o}$), which suggests that $6\mathbf{o}$ ($7\mathbf{o}$) was converted into $6\mathbf{c}$ ($7\mathbf{c}$) by oxidation.

This oxidative $6\mathbf{o}$ to $6\mathbf{c}$ cyclization is further supported by UV-vis spectroscopy, where the unique catalytic nature of the $6\mathbf{o}$ to $6\mathbf{c}$ isomerization was revealed by monitoring the change of the absorbance after adding 0.3 equiv. of $[(4\text{-BrC}_6\text{H}_4)_3\text{N}][\text{SbCl}_6]$ to a dichloromethane solution of $6\mathbf{o}$ (Figure 7A). The spectrum obtained at 2 hours after the addition of the oxidant was similar to that expected for $6\mathbf{c} + 6\mathbf{c}^+$ with the $6\mathbf{c}^+/6\mathbf{c}$ ratio of ca. 3/7, indicating that most $6\mathbf{o}$ were converted into $6\mathbf{c}$ (Figure 7B). The reaction rate of the electro-catalytic $6\mathbf{o}$ to $6\mathbf{c}$ isomerization was remarkably faster than that of (non-catalytic) thermal $6\mathbf{o}$ to $6\mathbf{c}$ isomerization which takes 4 days to terminate the isomerization.

The mechanism of the catalytic $6\mathbf{o}$ to $6\mathbf{c}$ isomerization is explained as follows (Figure 5): $6\mathbf{o}$ is oxidized by $[(4\text{-BrC}_6\text{H}_4)_3\text{N}][\text{SbCl}_6]$ to form $6\mathbf{o}^+$ (eq. 1). $6\mathbf{o}^+$ is thermally unstable to isomerize immediately to $6\mathbf{c}^+$ (eq. 2). Then, intermolecular electron transfer occurs from $6\mathbf{c}^+$ to neutral $6\mathbf{o}$, yielding neutral $6\mathbf{c}$ and $6\mathbf{o}^+$ (eq. 3). The generated $6\mathbf{o}^+$ isomerizes to $6\mathbf{c}^+$ according to eq. 2. Consequently, the chemical reactions shown in eq. 2 and eq. 3 successively occur so as to convert all $6\mathbf{o}$ into $6\mathbf{c}$. To confirm the reaction shown in eq. 3, 0.3 equiv. of $6\mathbf{c}^+$ was added to the solution of $6\mathbf{o}$, and the reaction was monitored by UV-vis spectroscopy. Predictably the absorbance of the peak derived from $6\mathbf{c}$ was increased, and eventually almost all $6\mathbf{o}$ was converted into $6\mathbf{c}$. This result supports the reaction in eq. 3, in which $6\mathbf{c}^+$

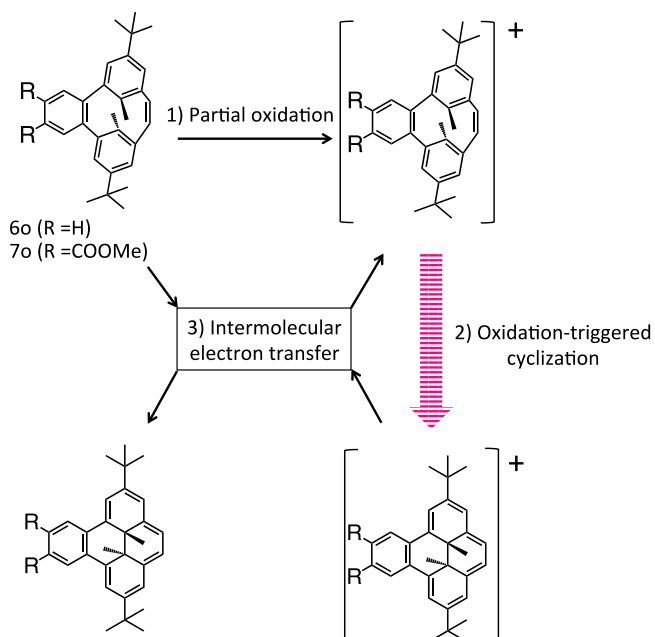


Figure 5. Scheme of the catalytic oxidation cyclization of 6 and 7 .

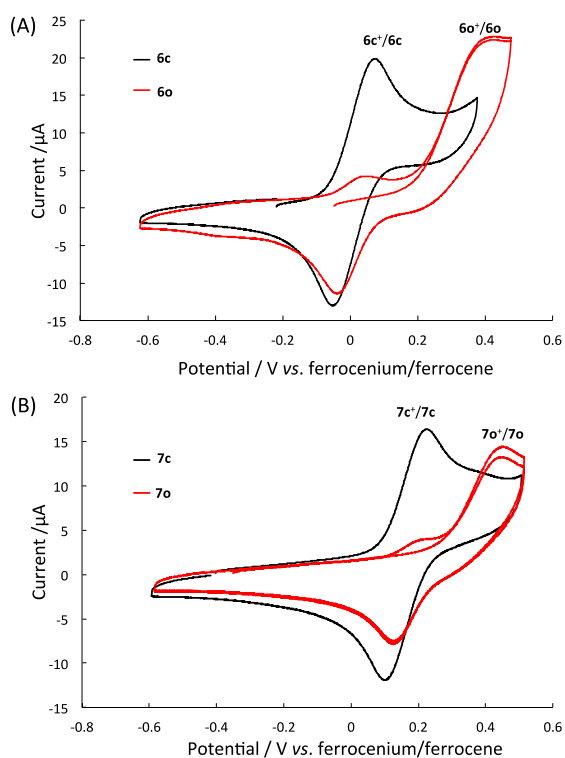


Figure 6. Cyclic voltammograms of $6\mathbf{c}$ and $6\mathbf{o}$ (A), and $7\mathbf{c}$ and $7\mathbf{o}$ (B), in 0.1 M Bu_4NClO_4 – dichloromethane.

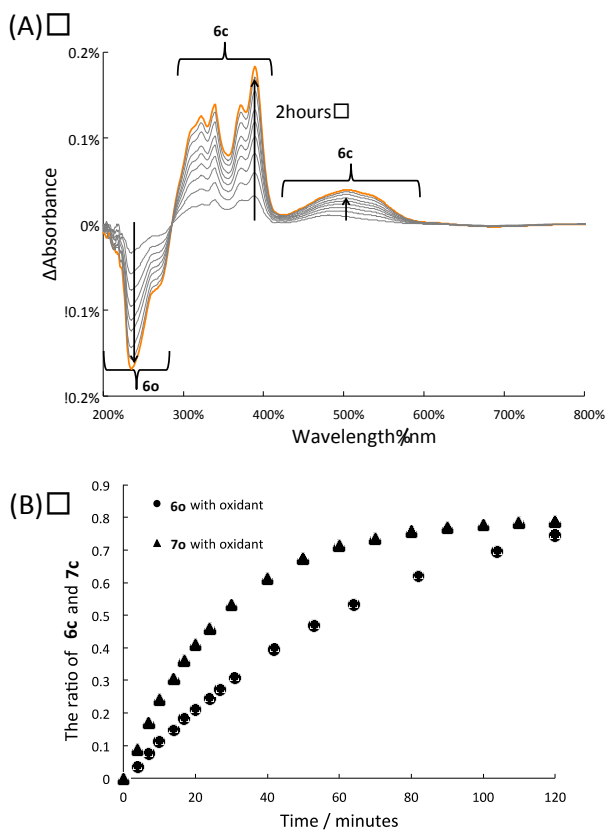


Figure 7. (A) Changes of Δ Absorbance after addition of 0.3 equivalent of $[(4\text{-BrC}_6\text{H}_4)_3\text{N}][\text{SbCl}_6]$ to 0.1 M dichloromethane solution of **1o**. Δ Absorbance indicates difference of spectrum from a spectrum just after the addition. (B) Time dependence of ratio of **1c** and **2c**.

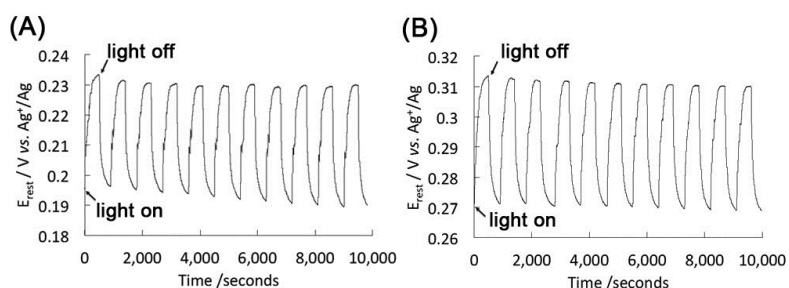


Figure 8. Change of electrode rest potential of (A) **6c** and (B) **7c** with 0.1 eq. of $[(4\text{-BrC}_6\text{H}_4)_3\text{N}][\text{SbCl}_6]$ in Bu_4NClO_4 -dichloromethane.

The results demonstrate a new photo-sensing system on the basis of the photoisomerization and electro-catalytic isomerization.

Conclusion

In my Ph.D study, I studied that electronic and photonic properties of DHP derivatives. It is found that DHP enhances the electronic communication between the redox sites, and that BzDHP derivative shows electro-catalytic isomerization. I fabricated reversible photo- and electro-responsive electrode system in chapter 3 and constructed a new photo-sensing system using this catalytic reaction in chapter 4. In this study, I proposed a new photo- and electro- functional system, which provides the basis to the construction of the functional molecular devices.

plays a key role in this chain reaction. The rate of the catalytic oxidative cyclization was higher in **6o** than in **6c**. $\Delta E_{\text{oxpeak}}^{0'}$ ($\Delta E_{\text{oxpeak}}^{0'}$ indicates the difference of $E_{\text{oxpeak}}^{0'}$ between **6o** (**7o**) and **6c** (**7c**)) is 0.10 V smaller in **7o** than in **6o**; thus, the intermolecular electron transfer shown in eq. 3 proceeds more efficiently in **7o** than in **6o**. The results were consistent with the expectation that the eq. 3 is a rate-determining step in the chain reaction.

The combination of the catalytic isomerization with the photochromic nature allowed me to establish a novel photo-sensing system. The introduction of photons (light signal) was detected by electrode rest potential (E_{rest} ; electric signal). In the presence of 0.1 equiv. of $\mathbf{6c}^+$, E_{rest} of the dichloromethane solution of **6c** was shifted from 0.20 V to 0.23 V vs. Ag^+/Ag by successive switching of the visible light irradiation (Figure 8A). This behavior was repeated over 10 cycles. E_{rest} is briefly determined by the $\mathbf{6c}^+/\mathbf{6c}$ ratio according to Nernst equation. The visible light irradiation converted **6c** into **6o** and increased the $\mathbf{6c}^+/\mathbf{6c}$ ratio. Eventually E_{rest} value was positively shifted. After

the irradiation was stopped, the catalytic **6o** to **6c** isomerization reaction was induced by the presence of $\mathbf{6c}^+$. Then the $\mathbf{6c}^+/\mathbf{6c}$ equilibrium reverted to the initial state to decrease E_{rest} to the initial value. As shown in Figure 8B, E_{rest} of **7c** was changed between 0.27 V and 0.31 V in the cycles. The range of E_{rest} was different from that of **6c**, while **6c** and **7c** were similar in ΔE_{rest} .